NEON ALGORITHM THEORETICAL BASIS DOCUMENT (ATBD) – 2D WIND SPEED AND DIRECTION

PREPARED BY	ORGANIZATION	DATE
Josh Roberti	FIU	12/04/2014
Stefan Metzger	FIU	12/20/2012
Sarah Streett	FIU	04/01/2014
Derek Smith	FIU	07/09/2013
Jesse Vance	AQU	02/09/2015

APPROVALS	ORGANIZATION	APPROVAL DATE
Kate Thibault	SCI	04/20/2022

RELEASED BY	ORGANIZATION	RELEASE DATE
Tanisha Waters	CM	04/20/2022

See configuration management system for approval history.

Change Record

REVISION	DATE	ECO #	DESCRIPTION OF CHANGE
A	08/29/2013	ECO-00935	Initial Release

B	10/23/2015	ECO-03110	Updated document to reflect L0 and L1 data product renumbering
			Revised *Algorithm Implementation* and *Uncertainty* Sections Added:
			  1. section regarding site-specific deviations of the North transducer head from True North
			  2. algorithms to compute distorted wind field, and
			  3. additional information regarding 'calm' winds.
			Added aquatic meteorology station information
			Removed dynamic calculations of effective degrees of freedom and implementing a standardized coverage factor of k=2 to calculate an expanded uncertainty at 95% confidence
			Added footnote to CVAL reference
			Moved mentions of Consistency analyses to the Future Updates Section in Each ATBD

C	04/20/2022	ECO-06809	• Revised logo • Revised fine print • Update to reflect change in terminology from relocatable to gradient sites • Added Neon to document title

TABLE OF CONTENTS

LIST OF TABLES AND FIGURES

1 DESCRIPTION

Contained in this document are details concerning wind measurements made at all NEON sites. Specifically, the processes necessary to convert "raw" sensor measurements into meaningful scientific units and their associated uncertainties are described. Wind will be continuously monitored by NEON at all core and gradient sites via 2- and 3-dimensional sonic anemometers; this document focuses on 2D sonic anemometers.

1.1 Purpose

This document details the algorithms used for creating NEON Level 1 (L1) data products (DPs) and ancillary data as defined in this document (such as calibration data) obtained via instrumental measurements made by the 2D sonic anemometers. It includes a detailed discussion of measurement theory and implementation, appropriate theoretical background, data product provenance, quality assurance and control methods, approximations and/or assumptions made, and a detailed exposition of uncertainty resulting in a cumulative reported uncertainty for this product.

1.2 Scope

The theoretical background and entire algorithmic process used to derive Level 1 data from Level 0 data for 2D anemometers are described in this document. The employed anemometers are Gill's Wind Observer II (WOII) and Extreme Weather Wind Observer (EWW0). The WOII has two versions: heated and non-heated; use of either will be site dependent throughout the Observatory. This document does not provide computational implementation details, except for cases where these stem directly from algorithmic choices explained here.

2   RELATED DOCUMENTS AND ACRONYMS

2.1   Applicable Documents

AD[01]	NEON.DOC.000001	NEON Observatory Design
AD[02]	NEON.DOC.005003	NEON Scientific Data Products Catalog
AD[03]	NEON.DOC.002652	NEON Level 1, Level 2, and Level 3 Data Products Catalog
AD[04]	NEON.DOC.005005	NEON Level 0 Data Products Catalog
AD[05]	NEON.DOC.002002	Engineering Master Location Sensor Matrix
AD[06]	NEON.DOC.011081	ATBD QA/QC plausibility tests
AD[07]	NEON.DOC.000783	ATBD De-spiking
AD[08]	NEON.DOC.000782	ATBD QA/QC Data Consistency
AD[09]	NEON.DOC.000746	Evaluating Uncertainty (CVAL)
AD[10]	NEON.DOC.000387	2D Wind Sensor Configuration, Command and Control
AD[11]	NEON.DOC.000785	TIS Level 1 Data Products Uncertainty Budget Estimation Plan
AD[12]	NEON.DOC.000784	ATBD Profile Development
AD[13]	NEON.DOC.000927	NEON Calibration and Sensor Uncertainty Values (CVAL)[1]
AD[14]	NEON.DOC.000902	2D Sonic Anemometer Validation Procedure (CVAL)
AD[15]	NEON.DOC.000387	2D Wind C^3 Document
AD[16]	NEON.DOC.001113	Quality Flags and Quality Metrics for TIS Data Products
AD[17]	NEON.DOC.001449	C^3 AQU 2D Wind Ultrasonic Anemometer

2.2   Reference Documents

RD[01]	NEON.DOC.000008	NEON Acronym List
RD[02]	NEON.DOC.000243	NEON Glossary of Terms

2.3   Acronyms and Variables

Acronym	Explanation
$\overline{A}$	Mean, minimum angular distance
A_i	Individual, minimum angular distance
$A_{i,c}$	Individual, corrected, minimum angular distance
A/D	Analog to Digital
ATBD	Algorithm Theoretical Basis Document
CVAL	NEON Calibration, Validation, and Audit Laboratory
DAS	Data Acquisition System
DP	Data Product
ENG	NEON Engineering department
EWWO	Gill's Extreme Weather Wind Observer 2D Sonic Anemometer
L0	Level 0

---

[1] Note that CI obtains calibration and sensor values directly from an XML file maintained and updated by CVAL in real time. This report is updated approximately quarterly such that there may be a lag time between the XML and report updates.

L1	Level 1
LHDD	Location Hierarchy Design Document
S	Wind Speed
U	Meridional (north – south) vector component
UQ	Unquantifiable uncertainty
V	Zonal (east – west) vector component
WOII	Gill's Wind Observer II Sonic Anemometer
θ	Wind Direction
θ_i	Individual wind direction θ_i
$\theta_{i,c}$	Individual, corrected angle (wind direction) measurement
$\bar{\theta}$	Mean, unit vector wind direction measurement
$\bar{\theta}_c$	Mean, corrected angle (wind direction) θ_i
$\bar{\bar{\theta}}_T$	Averaged wind direction; T denotes averaging period
θ_{T,σ^2}	Wind direction variance; T denotes averaging period

2.4   Verb Convention

"Shall" is used whenever a specification expresses a provision that is binding. The verbs "should" and "may" express non-mandatory provisions. "Will" is used to express a declaration of purpose on the part of the design activity.

3   DETAILED DESCRIPTION

3.1   Variables Reported

A suite of L1 data products will be produced by the algorithms displayed within this document. Statistical summaries associated with wind direction will only be that of variance; *values of minimum and maximum wind directions are misleading and are therefore not included as data products*.

Two-dimensional wind related L1 DPs provided by the algorithms documented in this ATBD are displayed in the accompanying file, tdw_datapub_NEONDOC002855.txt.

3.2   Input Dependencies

The L0 data used to produce L1 wind DPs are shown in **Table 1**.

Table 1. List of L0 DPs from 2D anemometer used to produce L1 wind DPs.

Description	Sample Frequency	Units	Data Product Number
U (North-South) vector component	1 Hz	m s^{-1}	NEON.DOM.SITE.DP0.00001.001.01306.HOR.VER.000
V (East-West) vector component	1 Hz	m s^{-1}	NEON.DOM.SITE.DP0.00001.001.01307.HOR.VER.000
Health Status of 2D wind speed sensor	1 Hz	NA	NEON.DOM.SITE.DP0.00001.001.01310.HOR.VER.000

3.3   Product Instances

Multiple 2D anemometers will be deployed at tower sites. These will be located on each boom arm below the top of the tower, oriented downward. A single 2D anemometer will be located at aquatic sites. This will be located at the top of the aquatic met station at a standard height of 3m above ground level, oriented upward.

3.4   Temporal Resolution

Two- and thirty-minute averages of wind speed and direction will be calculated to form L1 DPs.

3.5   Spatial Resolution and Extent

Each 2D anemometer will represent the point at which it is placed on the tower infrastructure. Ultimately, wind speed and direction profiles will be developed for each tower site from the array of 2D anemometers on the tower (see AD[05] for detail on sensor placement for a specific core site, and AD[12] for description of the algorithms used for deriving this profile).

4 SCIENTIFIC CONTEXT

Wind plays an important role in atmospheric and environmental sciences. A function of differential heating of Earth's surface and subsequent pressure gradients, horizontal and vertical winds are responsible for advection of atmospheric pollutants, moisture, heat and momentum (Stull 1988). As such, horizontal and vertical winds will be measured throughout the Observatory. This document details the processes by which mean horizontal wind is derived.

4.1 Theory of Measurement

Two-dimensional sonic anemometry relies on two pairs of transducers that measure wind velocity along orthogonal axes. As an example, to measure the north-south or east-west wind velocity (**Figure 1**), sound pulses are simultaneously emitted from two transducers that are placed a set distance apart (L). The times taken (T_1, T_2) for the ultrasonic pulses to travel along their respective axis to the far transducer head are recorded (Gill 2005) and wind velocities (i.e. zonal and meridional vector components) are

Figure 1. Ultrasonic anemometer theory (directionless) (Gill 2007).

then calculated from the differences in flight times across each axis (Brock and Richardson 2001; Gill 2005). This process is completed for the east–west and north-south axes independently. Wind velocity along each axis is computed as follows:

$$V_i = \frac{L_V}{2}\left(\frac{1}{T_{1_i}} - \frac{1}{T_{2_i}}\right) \tag{1}$$

and

$$U_i = \frac{L_U}{2}\left(\frac{1}{T_{3_i}} - \frac{1}{T_{4_i}}\right) \tag{2}$$

where:

T_{1_i} & T_{2_i}, T_{3_i} & T_{4_i} = Individual (1 Hz) transit times of ultrasonic pulses between the east-west and north-south transducer faces, respectively
L = Distance between transducer faces
U_i = Individual meridional (N-S) velocity (Figure 2)
V_i = Individual zonal (E-W) velocity (Figure 2).

Note that **Figure 1** is for illustration purposes only, the notation is not intended to match that of Eqns. (1) and (2).

Gill's 2D anemometers have an internal Analog to Digital (A/D) converter. Thus, NEON's Data Acquisition System (DAS) will acquire 1-Hz vector components in digital form.

4.2   Theory of Algorithms

The following sections describe the theory and implementation of algorithms for 2D sonic anemometer measurements.

4.2.1   Wind Speed

The magnitude of the horizontal wind speed (S_i) will be calculated for each 1 Hz, Level 0 datum, in accordance with the Pythagorean Theorem:

$$S_i = \left(U_i^2 + V_i^2\right)^{\frac{1}{2}} \tag{3}$$

After the vector components are converted to horizontal wind speed, two-minute ($\bar{S}_2$) and thirty-minute ($\bar{S}_{30}$) averages of horizontal wind speed will be determined accordingly to create the L1 wind-speed DPs listed in tdw_datapub_NEONDOC002855.txt:

$$\bar{S}_2 = \frac{1}{n} \sum_{i=1}^{n} S_i \tag{4}$$

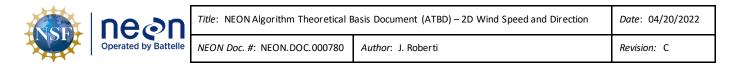where, for each two-minute average, *n* is the number of measurements during the averaging period and S_i is a 1-Hz horizontal wind speed measurement taken during the 120-second averaging period [0, 120). For a 2-minute average, *n* =120 if all data points are included.

Similarly,

$$\bar{S}_{30} = \frac{1}{n} \sum_{i=1}^{n} S_i \tag{5}$$

where, for each thirty-minute average, *n* is the number of measurements during the averaging period [0, 1800) and S_i is a 1-Hz horizontal wind speed measurement during the averaging period.
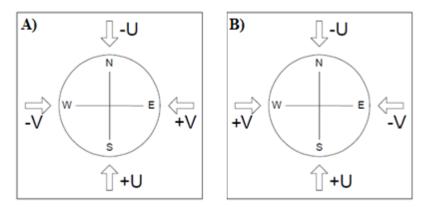
Note: The beginning of the first averaging period in a series shall be the nearest whole minute less than or equal to the first timestamp in the series.
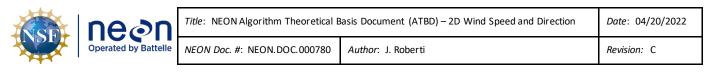
4.2.2 Wind Direction

Wind direction is typically indicated in terms of degrees from true north in the clockwise direction; e.g., 90° indicates a wind blowing from the east and 180° a wind blowing from the south, etc. In addition, 0° is used to indicate no (measurable) wind whereas 360° indicates a northerly wind.

Figure 2A shows the polarity of U and V for the upright installation of Gill's anemometer at aquatic sites assuming that the wind components along the U and V axes are blowing in the direction of the respective arrows. Thus, when U_i is negative and V_i is positive, the direction of the wind is between north and east. Because all of the Gill's 2D anemometers will be positioned upside down on the towers at terrestrial sites (refer to AD[10]), the zonal plane is essentially flipped (**Figure 2B**). With an upside-down installation, the wind direction is between north and east when both U_i and V_i are negative.

Figure 2. A) Coordinate system of an upright sonic anemometer (Gill 2007, 2011) used at Aquatic Sites; B) coordinate system of Gill's 2D sonic anemometer oriented upside-down used at Terrestrial Sites - it is important to note that the zonal plane is flipped because one of the transducer arms must be aligned with True North during installation.

The most direct calculation of wind direction employs the arctan2 function. In this case, the coordinate systems represented in **Figures 2A** and **2B** must be aligned with the standard Cartesian system, which measures angles counter-clockwise from the positive *x*-axis. Each coordinate system must be transformed such that the winds from the north, east, south and west are aligned with 360°, 90°, 180° and 270°, respectively, on the Cartesian system. To re-align, both **Figures 2A** and **2B** are rotated about the vertical axis and then rotated clockwise 90° so that the positive *x*-axis is in alignment with North and the positive *y*-axis with East. The transformation of **Figure 2A** results in the positive x-axis being aligned with –U vector and the positive y-axis being aligned with the +V vector. The transformation of Figure 2B results in the positive x-axis being aligned with the –U vector and the positive y-axis being aligned with the –V vector. These are shown in **Figure 3A** and **B** respectively.

Figure 3. A) Transformed coordinate system of an upright sonic anemometer used at Aquatic Sites; B) transformed coordinate system of sonic anemometer oriented upside-down used at Terrestrial Sites.

The benefit of this re-alignment is the ease with which the wind direction can be computed using the atan2 function. The atan2 function takes into account the sign of both vectors and places the angle in the correct quadrant. However the results are in the range (-π, π]. This can then be mapped to [0,2π) by adding 2π and performing the modulo operation of 2π. The sign of the U and V vectors must be changed for sensors deployed at both aquatic and terrestrial sites in order to have the resultant angle, θ, align with the *meteorological coordinate system.* Equations 6 and 7 are to be used for the Aquatic and Terrestrial sites respectively:

$$\theta_i = \begin{cases} 2\pi & \text{if } U_i < 0 \ \& \ V_i = 0, \\ [2\pi + \text{atan2}(V_i, -U_i)] \text{ modulo } 2\pi & \text{otherwise.} \end{cases} \tag{6}$$

$$\theta_i = \begin{cases} 2\pi & \text{if } U_i < 0 \ \& \ V_i = 0, \\ [2\pi + \text{atan2}(-V_i, -U_i)] \text{ modulo } 2\pi & \text{otherwise.} \end{cases} \tag{7}$$

where θ_i is the individual wind speed angle given in radians according to the *meteorological coordinate system*.

Note: The atan2 function in Eq. (6) assumes the following definition:

$$\text{atan2}(y,x) = \begin{cases} \arctan\left(\dfrac{y}{x}\right) & x > 0 \\ \arctan\left(\dfrac{y}{x}\right) + \pi & y \geq 0, x < 0 \\ \arctan\left(\dfrac{y}{x}\right) - \pi & y < 0, x < 0 \\ +\dfrac{\pi}{2} & y > 0, x = 0 \\ -\dfrac{\pi}{2} & y < 0, x = 0 \\ 0 & y = 0, x = 0 \end{cases} \tag{8}$$

Because some programs, i.e., Excel, reverse the arguments of the atan2 function (the first argument is placed in the denominator when calculating arctan), care must be taken in assigning the proper arguments to the atan2 function.

The inverse tangent function can also be used to calculate wind direction, but this method is not as straightforward. This is due to the fact that the inverse tangent function has a single argument and therefore does not take into account the individual signs of the U and V components. Also, the range of $\tan^{-1}$ is restricted to $\left(-\dfrac{\pi}{2}, \dfrac{\pi}{2}\right)$ so that separate definitions for winds from the east and west are required. These corrections are already built into the atan2 function (see Eq. (8)).

If the inverse tangent function is used, the individual wind direction, θ_i, is calculated for each Level 0 datum as follows:

$$\theta_i = \begin{cases} \left[2\pi + \tan^{-1}\left(\dfrac{V_i}{U_i}\right)\right] \text{ modulo } 2\pi & \text{if } U_i < 0, V \neq 0 \\ 2\pi & \text{if } U_i < 0, V_i = 0 \\ \dfrac{\pi}{2} & \text{if } U_i = 0, V_i < 0 \\ \dfrac{3\pi}{2} & \text{if } U_i = 0, V_i > 0 \\ 0 & \text{if } U_i = 0, = V_i \\ \tan^{-1}\left(\dfrac{V_i}{U_i}\right) + \pi & \text{if } U_i > 0 \end{cases} \tag{9}$$

Originally, the North transducer head of all 2D anemometers on towers was to be aligned with True North. However, this requirement has since changed at tower sites, and the North transducer head of all anemometers at a given NEON site will be aligned with the boom arms. The aquatic met station design allows the North transducer head of the 2D anemometer to be aligned with True North at all aquatic

sites and therefore will not need a directional correction. At terrestrial sites a site-specific correction C, from True North will be provided by NEON Systems Engineering (SE) and stored in the Cyberinfrastructure (CI) data store. Each 2D wind direction measurement will be corrected for this deviation from True North (Eq. (10)) after undergoing previous coordinate rotations.

$$\theta_i^{'} = [\theta_i - (2\pi - C)] \quad \text{modulo } 2\pi \tag{10}$$

Note that in either case, wind direction is calculated independently of wind speed.

Calculating the mean and variance of 2D wind direction is complicated by the fact that wind direction is a periodic variable with a discontinuity at 2π. For periods in which observations are i) dispersed across the discontinuity (2π) or ii) vary more than 180°, direct calculation of the arithmetic mean and variance is misleading. Consequently, an alternative approach is required for an exact solution. Here we follow an analytical two-pass method; this is a simple formulation with a theoretical basis that has been thoroughly reviewed (*e.g.,* Yamartino 1984; Mori 1986; Weber 1997; Farrugia *et al.* 2009).

In the first pass, the components of the average distance vector over an observation period with sample size *n* are calculated

$$\bar{Y} = \frac{1}{n}\sum_{i=1}^{n} \sin{(\theta_i')} \tag{11}$$

$$\bar{X} = \frac{1}{n}\sum_{i=1}^{n} \cos{(\theta_i')} \tag{12}$$

where, for each two-minute average, *n* represents the number of measurements in the averaging period [0, 120) seconds. Similarly, for each thirty-minute average, *n* represents the number of measurements in the averaging period [0, 1800) seconds.

Note: The beginning of the first averaging period in a series shall be the nearest whole minute less than or equal to the first timestamp in the series.

Note: The average *vector* components $\bar{X}$ and $\bar{Y}$ differ from the *average wind vector* components in that they *are not weighted* by the wind magnitude of the individual, corresponding wind speed, S_i.

Next, the *unit-vector mean wind direction* is derived (e.g., Yamartino 1984) using the atan2 function:

$$\bar{\theta} = \begin{cases} 2\pi & \text{if } \bar{X} > 0 \,\&\, \bar{Y} = 0, \\ [2\pi + \text{atan2}(\bar{Y}, \bar{X})] \bmod (2\pi) & \text{otherwise.} \end{cases} \tag{13}$$

Again, care must be taken when assigning arguments to the atan2 function as discussed above.

Alternatively, the arc tangent function can be used with the appropriate corrections:

$$\bar{\theta} = \begin{cases} \left[2\pi + \tan^{-1}\left(\dfrac{\bar{Y}}{\bar{X}}\right) \right] \text{ modulo } 2\pi & \text{if } \bar{X} \neq 0 \\ \dfrac{\pi}{2} & \text{if } \bar{Y} > 0 \ \& \ \bar{X} = 0 \\ \dfrac{3\pi}{2} & \text{if } \bar{Y} < 0 \ \& \ \bar{X} = 0 \\ 0 & \text{if } \bar{X} = \bar{Y} = 0 \end{cases} \tag{14}$$

where $\bar{\theta}$ is the mean unit vector wind direction in radians.

In the second pass, the *minimum angular distance* (A_i) between an observation and the mean is calculated (Batschelet, 1981):

$$A_i = \left| \cos^{-1}\left(\cos(\theta_i - \bar{\theta}) \right) \right|. \tag{15}$$

Subsequently the sign of the minimum angular distance is determined (Farrugia *et al.* 2009):

$$A_{i,c} = \begin{cases} A_i & \text{if} \quad \bar{\theta} \leq \theta_i < (\bar{\theta} + \pi), \\ -A_i & \text{if} \quad (\bar{\theta} - \pi) < \theta_i < \bar{\theta}, \end{cases} \tag{16}$$

where, $A_{i,c}$ is the individual, corrected, minimum angular distance between subsequent measurements.

Next, the average over all $A_{i,c}$ can be calculated *with an expected value of zero for symmetric angular distributions*:

$$\bar{A}_T = \frac{1}{n} \sum_{i=1}^{n} A_{i,c}. \tag{17}$$
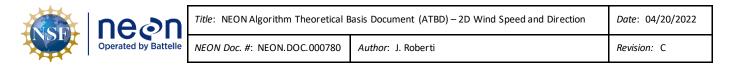
Where, for each two-minute average, *n* is the number of measurements in the averaging period, [0,120) seconds. For each thirty-minute average, *n* is the number of measurements in the averaging period [0, 1800) seconds. Again, the beginning of the first averaging period in a series shall be the nearest whole minute less than or equal to the first timestamp in the series.

The arithmetic mean is defined such that it minimizes the sample variance. If the angular distribution is skewed, $\bar{A}_T$ is exactly the difference between the arithmetic mean wind direction and the unit-vector mean wind direction. With respect to the arithmetic mean, $A_{i,c}$ are thus overestimated by $\bar{A}_T$; this discrepancy is compensated for to yield the arithmetic mean and variance:

$$\bar{\theta}_T' = (\bar{\theta} + \bar{A}_T)\text{ modulo } 2\pi \tag{18}$$

The sample variance of wind direction is calculated as follows (Yamartino, 1984):

$$s^2(\bar{\theta}_T') = \left(n^{-1} \sum_i (A_{i,c})^2 - (\bar{A}_T)^2 \right). \tag{19}$$

Finally the resulting angles are converted from radians to angular degree to create the L1 wind-direction DPs listed in tdw_datapub_NEONDOC002855.txt:

$$\bar{\theta}_T = \bar{\theta}_T' \cdot \frac{180}{\pi} \tag{20}$$

and

$$s^2(\bar{\theta}_T) = s^2(\bar{\theta}_T') \cdot \frac{180}{\pi} \tag{21}$$

where the subscript *T* represents either 2 (two-minute average) or 30 (thirty-minute average).

5   ALGORITHM IMPLEMENTATION

Data flow for signal processing of L1 DPs will be treated in the following order.
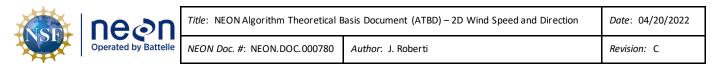
1.   Incoming 1 Hz U and V wind components will be stored as level 0 data
2.   <u>WIND SPEED</u>:
     a.   The L0 vector data will be converted to horizontal wind speed via Eq. (3).
     b.   QA/QC Plausibility tests will be applied to each scalar wind speed datum in accordance with AD[06]. The details are provided in Section 5.1.
     c.   Average (two and thirty-minute), horizontal wind speeds will be calculated using Eq. (4) and (5)
           i.   A post-averaging check will take place on two and thirty-minute *wind speed* averages (see Section 5.1)
     d.   Descriptive statistics, i.e., minimum, maximum, and variance, of wind speed will be determined for both two- and thirty-minute averages.
     e.   Quality metrics, quality flags, and the final quality flag will be produced for two- and thirty-minute averages according to AD[16].
3.   <u>WIND DIRECTION</u>:
     a.   The L0 U and V vector components will be converted to wind direction (radians) via Eq. (6) and (7) for Aquatic and Terrestrial Sites respectively.
     b.   Limited QA/QC Plausibility tests will be applied to each wind direction datum in accordance with AD[06]; details are provided in Section 5.1.
     c.   Two- and thirty-minute average, unit vector wind directions will be calculated using equations (11) through (21).
     d.   Variance of wind direction will be calculated for both two- and thirty-minute averages
     e.   Quality metrics, quality flags, and the final quality flag will be produced for two- and thirty-minute averages according to AD[16].

5.1   QA/QC Procedure

1.   <u>Plausibility tests</u> AD [06] – All plausibility tests with the exception of the step test will be determined for wind speed and direction. Unless otherwise noted all plausibility tests will be applied to the converted L0 DPs, and associated quality flags (QFs) will be generated for each test. Test parameters will be provided by FIU and maintained in the CI data store.
     a)   <u>Range Test</u> – Many NEON sites reside in forested areas. Obstructions (*e.g.,* tower infrastructure, trees and/or flora) upstream of the anemometer can cause distortion to the wind flow (Dyer 1980; WMO 2008). Although the wind measurements made at many sites will be affected by distorted wind flow resulting from upstream obstruction of living objects, only wind measurements obstructed by inanimate objects (*i.e.,* tower infrastructure) will be flagged. To denote instances when wind flow has been distorted by an *inanimate object*

prior to measurement, a flag: QF_θ, will be applied to i) wind speed and ii) wind direction measurements. Data will be flagged as a function of site-specific derived thresholds.

SE will provide i) site-specific x-y coordinates representing the spatial extent of tower obstructions; ii) the boom orientation of the 2D anemometer (relative to True North); iii) x-y coordinate of the 2D anemometer. The x-y coordinates shall correspond to a right-hand Cartesian coordinate system, relative to the 2D anemometer boom. In other words, the (0,0) position of the x-y coordinate system shall always reside at the tower corner, or base point, of the 2D anemometer's boom, and the positive x axis of the coordinate system shall always correspond to the 2D anemometer boom, such that the position of the 2D anemometer at each site resides at (L,0; see **Figure 4**).

Figure 4. An example of the Cartesian coordinate system as used to calculate site-specific, distorted wind flow regions. The tower is shown as a gray square; the coordinate system is represented by the black lines; the 2D anemometer boom is given as a red line and the 2D anemometer is displayed as a black star. True North is denoted at the top of the Figure.

Site-specific distorted wind flow thresholds shall be derived with the provided data and via the following equations. The lower and upper bounds of the distorted wind field are first calculated relative to the Cartesian coordinate system.

$$c_d = \frac{\left| \tan^{-1}\left(\frac{y_c}{L + |x_c|} \right) \right| * 180}{\pi} \tag{22}$$

$$cc_d = \frac{\left| \tan^{-1}\left(\frac{y_{cc}}{L + |x_{cc}|} \right) \right| * 180}{\pi} \tag{23}$$

Where,
c_d = angle of distorted flow clockwise from the 2D anemometer boom (degrees)

cc_d = angle of distorted flow counter-clockwise from the 2D anemometer boom (degrees)

L = X coordinate of the 2D anemometer; Y coordinate shall always = 0

x_c = X coordinate of tower obstruction extent clockwise from 2D anemometer's boom

y_c = Y coordinate of tower obstruction extent clockwise from 2D anemometer's boom

x_{cc} = X coordinate of tower obstruction extent counter-clockwise from 2D anemometer's boom

y_{cc} = Y coordinate of tower obstruction extent counter-clockwise from 2D anemometer's boom

Next, buffer zones are added and the upper and lower bounds of the distorted wind field are corrected to True North.

$$D_{min} = [O_{2D} - (c_d + B_{min}) + 180] \text{ modulo } 360 \qquad (24)$$

$$D_{max} = [O_{2D} + (cc_d + B_{max}) + 180] \text{ modulo } 360 \qquad (25)$$

Where,

D_{min} = distorted flow minimum threshold (relative to True North; degrees)

D_{max} = distorted flow maximum threshold (relative to True North; degrees)

O_{2D} = Boom arm orientation (relative to True North; degrees)

B_{min} = buffer to be applied to minimum threshold (degrees)

B_{max} = buffer to be applied to maximum threshold (degrees)

5.2 Post-averaging Check

To verify the plausibility of reporting wind direction as a numeric value, the following post-averaging check must be implemented.

The Office of the Federal Coordinator for Meteorology (OFCM) (2005) notes that wind directions derived from calm winds (specifically – wind speeds ≤ 6 kts (~3.0 m s^{-1})) are unreliable. The World Meteorological Organization (WMO) (2008) also acknowledges this relationship, but states a lower threshold – wind speeds ≤ 0.5 m s^{-1}. To insure international traceability, we will abide by the standard set forth by the WMO (2008). Thus, two and thirty-minute averaged wind speed data will undergo a post-averaging check to determine if their value is ≤ 0.5 m s^{-1}. In the event that the average wind speed is ≤ 0.5 m s^{-1}, *wind direction* for the same averaging period shall be flagged (QF_c).

5.3 Sensor Test

Gill's 2D anemometers produce error codes that accompany raw U and V vector measurements. These codes will result in the generation of a flag. For example, if the 2D anemometer displays an error code of '10' (refer to AD[15]), the sensor is informing the user that inaccurate data are likely being output because of a system gain max. In any case, data accompanied by error codes will be denoted by the following error flag:

$$QF_E = \begin{cases} 1 & \text{If raw datum is accompanied by error code} \\ 0 & \text{otherwise.} \end{cases}$$

In the event that a sensor health status code is generated, i.e., $QF_E = 1$, data will not be used to calculate the L1 mean data product.

5.4   Signal De-spiking

Signal de-spiking will not be conducted with wind speed or direction.

5.5   Quality Flags (QFs) and Quality Metrics (QMs) AD[16]

If a datum has failed one of the following tests it will not be used to create a L1 DP, **sensor test**. α and β QFs and QMs will be determined using the flags in **Table 2**. In addition, L1 DPs will have a QA/QC report and quality metrics associated with each flag listed in **Table 2** as well as a final quality flag, as detailed in AD[16]. Ancillary information needed for the algorithm and other information maintained in the CI data store is shown in **Table 3**.

Table 2. Flags associated with 2D wind measurements.

Flags
Null
Gap
Distorted flow
Sensor Test AD[15]
Consistency Analysis
Calm winds
Final quality flag

Table 3. Information maintained in the CI data store for 2D wind.

Tests/Values	CI Data Store Contents
Null	Test limit
Gap	Test limit
Calibration	CVAL sensor specific calibration coefficients
Uncertainty	AD[13]
Sensor Test	AD[15]
Final Quality Flag	AD[16]

6   UNCERTAINTY

Uncertainty of measurement is inevitable (JCGM 2008, 2012; Taylor 1997). It is crucial that uncertainties are identified and quantified to determine statistical interpretations about mean quantity and variance structure; both are important when constructing higher level data products (e.g., L1 DP) and modeled processes. This portion of the document serves to identify, evaluate, and quantify sources of uncertainty relating to L1 mean DPs. It is a reflection of the information described in AD[11], and is explicitly described for the 2D wind assembly in the following sections.

6.1   Uncertainty of wind measurements

Uncertainty of the 2D wind assembly is discussed in this section. Sources of uncertainties include those arising from vector component measurements, measurement noise, heater, resolution of the digital indication, and orientation to True North (**Figure 4**).
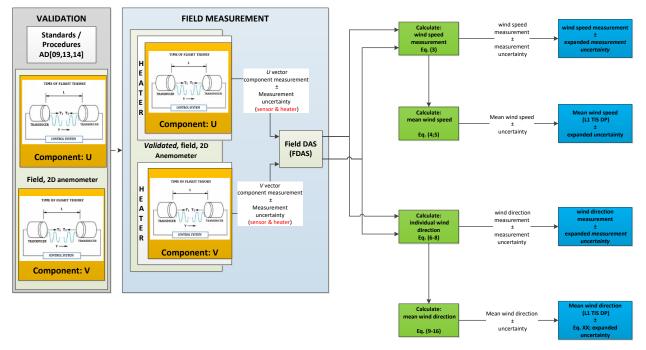

Figure 5. Diagram outlining potential sources of uncertainty associated with 2D wind L1 DPs. The salmon colored boxes represent the direct measurement of vector velocity based on the theory of sonic anemometry. For more information regarding the validation procedure, please refer to AD[09,13,14]

6.1.1   Validation

CVAL will not calibrate Gill's 2D anemometers, and will only be validating them. No measurement uncertainty values will be supplied by CVAL because of this. Measurement uncertainties must therefore be derived through a combination of manufacturer's specifications and scientific judgment; for further justification please refer to AD[11].

6.1.2   Accuracy

Gill does not provide accuracy values for individual vector components, but supplies them for horizontal wind speed (**Table 4**) and direction (±2° = 0.0349 radians). Despite the fact that Gill provides values of accuracy for horizontal, scalar wind speed and direction, our L0 data are in vector component form. Therefore, individual vector component uncertainties must be estimated from the provided wind speed accuracy.

Table 4. Relationship between wind speed and accuracy. It should be noted that these accuracies are related to horizontal wind speed and not individual vector component magnitude (Murree Sims, personal communication, Gill Instruments, 2012).

Wind Speed (m s^{-1})	Accuracy (± %)
0.01[1]	1.0
5	1.0
12	2.0
32	3.0
65	4.0
70[2]	4.0
[1]Starting threshold of Gill's 2D anemometers. It is assumed here that the accuracy of measurement is ± 1 % [2]Only applicable with the EWWO	

Linear interpolation is used to determine accuracy values between the limits provided in **Table 4**.

A.   [0.01, 5) m s^{-1}

$$u(S_i) = C_{m1}S_i - C_{b1} \quad [m\,s^{-1}] \tag{26}$$

B.   [5, 12) m s^{-1}

$$u(S_i) = C_{m2}S_i - C_{b2} \quad [m\,s^{-1}] \tag{27}$$

C.   [12, 32) m s^{-1}

$$u(S_i) = C_{m3}S_i - C_{b3} \quad [m\,s^{-1}] \tag{28}$$

D.   [32, 65) m s^{-1}

$$u(S_i) = C_{m4}S_i - C_{b4} \quad [m\,s^{-1}] \tag{29}$$

E.   [65, 70] m s^{-1}

$$u(S_i) = C_{m5}S_i - C_{b5} \quad [m\,s^{-1}] \tag{30}$$

Where:

$u(S_i)$ = Uncertainty (i.e., accuracy; Gill 2007, 2011) of individual wind speed S_i

S_i = individual (1 Hz) wind speed as calculated with Eq. (3).

C_{m1} = 0.0100

C_{b1} = 0.0

C_{m2} = 0.0271

C_{b2} = 0.0857

C_{m3} = 0.036

C_{b3} = 0.1920

C_{m4} = 0.0497

C_{b4} = 0.6303

C_{m5} = 0.0400

C_{b5} = 0.0

From here, the individual vector component measurement uncertainties can be derived with the aid of the wind speed information provided by Gill (2007, 2011). To do so requires the assumption that the north-south and east-west wind velocity component measurements are independent and that they contribute to the uncertainty of a wind speed measurement in proportion to their magnitude.

Under these assumptions, the uncertainties of the velocity component measurements can be calculated as follows:

$$u(U_i) = \begin{cases} \dfrac{1}{\sqrt{2}} \cdot u(S_i), & U_i = V_i = 0 \\ \sqrt{\dfrac{U_i^2}{U_i^2 + V_i^2}} \cdot u(S_i), & \text{otherwise} \end{cases} , \quad [m\,s^{-1}] \quad (31)$$

and

$$u(V_i) = \begin{cases} \dfrac{1}{\sqrt{2}} \cdot u(S_i), & U_i = V_i = 0 \\ \sqrt{\dfrac{V_i^2}{U_i^2 + V_i^2}} \cdot u(S_i), & \text{otherwise} \end{cases} \quad [m\,s^{-1}] \quad (32)$$

6.1.3 Resolution of the digital indication

As noted by Gill (2007, 2011), their 2D anemometers have a digital resolution of 0.01 m s^{-1}. Given that it is reasonable to assume the value of the measurand lies with equal probability between the bounds of this resolution, and it is unlikely that it resides outside these bounds, we can assume a uniform distribution (ISO1995) with related uncertainty (standard deviation) of:

$$u(R) = \frac{0.01\,\text{m s}^{-1}}{\sqrt{3}} = \pm\, 0.0058 \quad [m\,s^{-1}] \quad (33)$$

6.1.4   DAS

Gill 2D anemometers have an internal Analog to Digital (A/D) converter and output data in digital form. Therefore, no data conversions occur within the DAS. Thus, uncertainty related to the DAS can be considered negligible.

6.1.5   Offset Error

It is reported by Gill (2007, 2010) that each measurement is accompanied with an *offset* error of ± 0.01 m s^{-1} to account for values near 0. This offset error is included in the accuracies stated in Table 6-1 (personal communication with Richard McKay).
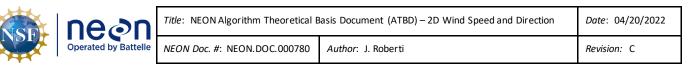
6.1.6   Heaters

Two models of Gill's sonic anemometers (EWWO and WOII: *version 2*) are equipped with heaters. These heaters warm the transducer heads if the ambient temperature drops below a certain threshold. The principles of sonic anemometry rely on the speed of sound, which is a function of temperature. It is hypothesized that this heating will cause small thermals around each transducer head, thus altering the neighboring temperature and causing uncertainty of the measurements. Because NEON *will not* calibrate these sensors in-house or monitor the current draw of the heaters, we cannot confidently determine the measurement uncertainty introduced by the heaters. However, we have been assured by Murree Sims (Gill Instruments, pers. comm. 2012) that heating will cause negligible uncertainty. Given the reassurance from the manufacturer, L1 Wind DPs will still be computed during instances when the heater is on.

6.1.7   Orientation

The 2D anemometer's orientation relative to true north is considered a source of uncertainty. A site-specific uncertainty value $u(O)$, will be provided by SYS ENG and stored in the CI data store.

6.1.8   Distorted Flow

As mentioned in Section 5.1, wind flows become distorted if subjected to obstructions (e.g., tower infrastructure) upstream of the anemometer (Dyer 1980; WMO 2008). Distorted flow introduces uncertainty that is a function of i) the obstructions upstream of the anemometer, ii) the magnitude of wind speed, and iii) characteristics of the wind (i.e., laminar vs. turbulent flow independent of upstream obstacles). Although previous researchers (e.g., Dyer 1980) have quantified the uncertainty associated with distorted flow, the obstructions upstream of our 2D anemometers differ from those utilized by previous researchers. Thus, it may be inappropriate to solely use their results as metrics to quantify the uncertainty introduced by distorted flow. As NEON data are analyzed, this topic will be further investigated and hopefully quantified. At current date, this is an uncertainty that can be identified, but not fully quantified; therefore, as mentioned in Section 5.1, the data will be flagged during instances of distorted flow.

6.1.9   Combined Measurement Uncertainty

The combined measurement uncertainties of the individual vector components can be estimated as follows:

$$u_c(V_i) = \left(u^2(V_i) + u^2(R)\right)^{\frac{1}{2}} \quad [m\,s^{-1}] \tag{34}$$

$$u_c(U_i) = \left(u^2(U_i) + u^2(R)\right)^{\frac{1}{2}} \quad [m\,s^{-1}] \tag{35}$$

The combined measurement uncertainty of individual wind speed observations is calculated as follows:

$$u_c(S_i) = \left(u^2(S_i) + u^2(R)\right)^{\frac{1}{2}} \quad [m\,s^{-1}] \tag{36}$$

The combined measurement uncertainty of an *individual,* valid (i.e., *those that are not flagged and omitted*) wind direction observation is:

$$u_c(\theta_i) = \left(0.0349^2 + u^2(O)\right)^{\frac{1}{2}} \quad [rad] \tag{37}$$

6.1.10   Expanded Measurement Uncertainty

The expanded measurement uncertainties are respectively calculated as:

$$U_{95}(V_i) = k_{95} * u_c(V_i) \tag{38}$$

$$U_{95}(U_i) = k_{95} * u_c(U_i) \tag{39}$$

$$U_{95}(S_i) = k_{95} * u_c(S_i) \tag{40}$$

$$U_{95}(\theta_i) = k_{95} * u_c(\theta_i) \tag{41}$$

Where:

$\quad U_{95}(Y_i)$ = respective expanded measurement uncertainty at 95% confidence

$\quad k_{95}$ = 2 (unitless); coverage factor for 95% confidence

6.2   Uncertainty of L1 DPs

The following subsections discuss uncertainties associated with L1 mean data products. It is important to note the differences between the *measurement uncertainties* presented in Section 6.1 and the uncertainties presented in the following subsections. The uncertainties presented in the following

subsections reflect the uncertainty of a time-averaged mean value, that is, they reflect the uncertainty of a distribution of measurements collected under non-controlled conditions (i.e., those found in the field), as well as any remaining uncertainties due to systematic errors related to the field assembly.

6.2.1 Wind Speed

6.2.1.1 Combined Uncertainty

The uncertainty of our L1 mean wind speed DPs is calculated from the sample variance of the measurements taken during the averaging period and the individual measurement uncertainties as follows:

$$u_{NAT}^2(\bar{S}) = \frac{\sum_{i=1}^{n} S_i^2}{n} - \bar{S}^2$$

$$u_c(\bar{S}) = \left(u_{NAT}^2(\bar{S}) + \frac{\sum_{i=1}^{n} u_c^2(S_i)}{n} \right)^{\frac{1}{2}} [m \, s^{-1}]$$

(42)

Note that this is likely to be a slight overestimate due to the fact that the variability in the measurements over the averaging period includes much of the uncertainty of an individual measurement. However, $u_c^2(S_i)$ is a Type B uncertainty and it is therefore not possible to extract uncertainty components. Practically speaking, any overestimate will be negligible.

6.2.1.2 Expanded Uncertainty

The expanded uncertainty is calculated as:

$$U_{95}(\bar{S}) = k_{95} * u_c(\bar{S})$$

(43)

Where:

$U_{95}(\bar{S})$ = expanded measurement uncertainty at 95% confidence (m s^{-1})
k_{95} = 2 (unitless); coverage factor for 95% confidence

6.2.2 Wind Direction

6.2.2.1 Combined Uncertainty

The overall uncertainty of the L1 mean wind direction DPs is calculated from the sample variance of the measurements taken during the averaging period and the individual measurement uncertainties as follows:

$$u_{NAT}^2(\bar{\theta}) = \frac{\sum_{i=1}^n \theta_i^2}{n} - \bar{\theta}^2$$

$$u_c(\bar{\theta}) = \left(u_{NAT}^2(\bar{\theta}) + \frac{\sum_{i=1}^n u_c^2(\theta_i)}{n}\right)^{\frac{1}{2}} \quad [rad]$$

(44)

Again, this is likely to be a slight overestimate due to the fact that the variability in the measurements over the averaging period includes much of the uncertainty of an individual measurement. However, $u^2(\theta_i)$ is a Type B uncertainty and it is therefore not possible to extract uncertainty components. Practically speaking, any overestimate will be negligible.

Note:
In the event that wind direction is presented as a non-numeric value (refer to Section 5.2), then combined and expanded uncertainty of wind direction will not be calculated.

6.2.2.2   Expanded Uncertainty

The expanded uncertainty is calculated as:

$$U_{95}(\bar{\theta}) = k_{95} * u_c(\bar{\theta})$$

(45)

Where:

$U_{95}(\bar{\theta})$ = expanded measurement uncertainty at 95% confidence (m s^{-1})
k_{95} = 2 (unitless); coverage factor for 95% confidence

6.3   Uncertainty Budget

The uncertainty budget is a visual aid detailing i) quantifiable sources of uncertainty, ii) means by which they are derived, and iii) the order of their propagation. Individual uncertainty values denoted in this budget are either provided here (within this document) or will be provided by other NEON teams (e.g., CVAL) and stored in the CI data store.

Table 5. Uncertainty budget for L1 Wind DPs. Shaded rows denote the order of uncertainty propagation (from lightest to darkest).

Source of uncertainty	Standard uncertainty component $u(x_i)$	Value of standard uncertainty	$c_i \equiv \dfrac{\partial f}{\partial x_i}$	$u_i(Y) \equiv \lvert c_i \rvert u(x_i)$
L1 Wind Speed DP	$u_c(\bar{S})$	Eq. (42) [m s^{-1}]	--	--
1 Hz Wind Speed	$u_c(S_i)$	Eq. (36) [m s^{-1}]	1	$u_c(S_i)$ [m s^{-1}]
1 Hz V component	$u_c(V_i)$	Eq. (34) [m s^{-1}]	n/a	n/a
Dig. Ind. Resolution	$u(R)$	Eq. (33) [m s^{-1}]	1	Eq. (33) [m s^{-1}]
1 Hz U component	$u_c(U_i)$	Eq. (35) [m s^{-1}]	n/a	n/a
Dig. Ind. Resolution	$u(R)$	Eq. (33) [m s^{-1}]	1	Eq. (33) [m s^{-1}]
L1 Wind Direction DP	$u_c(\bar{\theta})$	Eq. (44) [rad]	--	--
1 Hz Wind Direction	$u_c(\theta_i)$	Eq. (37) [rad]	1	Eq. (37) [rad]
Orientation	$u(O)$	Eq. (33) [rad]	1	Eq. (33) [rad]

7 FUTURE PLANS AND MODIFICATIONS

Quantification of sensor drift may be added into the uncertainty section of this document.

QA/QC tests may be expanded to include consistency analyses among similar measurement streams. A QA/QC flag for data consistency will be applied to data from terrestrial sites according to the consistency analysis outlined in AD[08], and a pass/fail flag will be generated to reflect this activity. Consistency analyses cannot be performed on wind data from aquatic sites. For 2D wind consistency analysis, L1 wind speed and direction data from a given anemometer will first be compared to the neighboring anemometer located above it on the tower infrastructure. If a statistical relationship between the two wind speed or direction measurements falls within defined limits provided by FIU (and maintained in the CI data store), then the sensor will pass the consistency analysis. Alternatively, a wind speed or direction difference outside the defined limits will result in a failed test. In this event of a failed test, the anemometer will then be compared to the neighboring anemometer located below it; if this too results in a failed test then the wind speed or direction data will fail the consistency analysis and be flagged as such. If the data fail the first test but pass the second, then they will pass the consistency analysis. This structure helps to ensures that non-functional sensors (e.g., sensors that are faulty or down for service) do not bias the test, since a resulting failed test will allow the sensor to be compared to the one below it. Accordingly, the 2D anemometer located on the bottom of the tower will only be compared to the neighboring anemometer located above it. The uppermost 2D anemometer will be compared to the anemometer below it and the 3D anemometer above it.

Note: Although this consistency analysis may be applicable for regions with homogeneous terrain, such an approach may not be applicable to regions of heterogeneous terrain and those where comparison anemometers are located above and below a canopy.

8   BIBLIOGRAPHY

Batchelet, E. (1981) Circular Statistics in Biology. Academic Press. 371 pp.

Brock, F. V., & Richardson S. J. (2001) *Meteorological Measurement Systems*. Oxford University Press, Inc. 290 pp.

Dyer, A. J. (1981) Flow distortion by supporting structures. *Boundary Layer Meteorology,* **20**, 243-251.

Environmental Protection Agency (EPA) (1990) Meteorological Monitoring Guidance for Regulatory Modeling Applications. [Available online at: http://www.epa.gov/scram001/guidance/met/mmgrma.pdf]

Environmental Protection Agency (EPA) (2002) Guidance on Environmental Data Verification and Data Validation. [Available online at: http://www.epa.gov/QUALITY/qs-docs/g8-final.pdf]

Farrugia, P. S., Borg, J. L., & Micallef A. (2009) Notes and Correspondence: On the Algorithms Used to Compute the Standard Deviation of Wind Direction. *Journal of Applied Meteorology*, **48**, 2144 – 2151.

Fisher, N. I. (1983) Comment on "A Method for Estimating the Standard Deviation of Wind Directions" by K. A. Verrall & Williams. R. L., *Journal of Applied Meteorology and Climatology*, **22**, 1971 – 1972.

Gill Instruments Ltd. (2007) *User Manual: WindObserver II Ultrasonic Anemometer*. Document # 1390-PS-004. Issue 17.

Gill Instruments Ltd. (2011) *User Manual: Extreme Weather WindObserver with Enhanced Heating Ultrasonic Anemometer*. Document # 1390-PS-0018. Issue 6.

Joint Committee for Guides in Metrology (JCGM) (2008) Evaluation of measurement data – Guide to the expression of uncertainty in measurement. pp. 120.

JCGM (2012) International vocabulary of metrology – Basic and general concepts and associated terms (VIM). 3rd Edition. pp. 92

Mori, Y. (1987) Methods for Estimating the Mean and the Standard Deviation of Wind Direction. *Journal of Applied Meteorology and Climatology*, **26**, 1282-1283.

Office of the Federal Coordinator for Meteorology (OFCM) (2005) Federal Meteorological Handbook: Surface Weather Observations and Reports – Wind, 3.1-3.5. [Available online at http://www.ofcm.gov/fmh-1/pdf/E-CH5.pdf]

Pearcy, R. W., Ehleringer J., Mooney H. A., & Rundel P. W. (1989) *Plant Physiological Ecology: Field Methods and Instrumentation*. Chapman and Hall, 457 pp.

Stull, R. B. (1988) An Introduction to Boundary Layer Meteorology. Kluwer Academic Press, 666 pp.

Taylor, B. N., & Kuyatt C. E. (1994) *Technical Note 1297: Guidelines for Evaluating and Expressing the Uncertainty of NIST Measurement Results*. United States National Institute of Standards and Technology. 20 pp

Taylor, J. R. (1997) *An Introduction to Error Analysis: The Study of Uncertainties in Physical Measurements*. University Science Books. 270 pp.

Weber, R. (1997) Estimators for the Standard Deviation of Horizontal Wind Direction. *Journal of Applied Meteorology and Climatology,* **36**, 1403 – 1415.

World Meteorological Organization (WMO) (2008) Measurement of Surface Wind. *Guide to Meteorological Instruments and Methods of Observations.* 8th Ed. I.5-1 – 1.5-14.

Yamartino, R. J. (1984) A Comparison of Several "Single-Pass" Estimators of the Standard Deviation of Wind Direction. *Journal of Applied Meteorology and Climatology*, **23**, 1362-1366.